Journal of Colloid and Interface Science 599 (2021) 79–87

Contents lists available at ScienceDirect

Journal of Colloid and Interface Science

journal homepage: www.elsevier.com/locate/jcis

Regular Article

Hydration of bromide at reverse micelle interfaces studied by X-ray absorption fine structure

Makoto Harada *, Hinako Sakai, Yu Fukunaga, Tetsuo Okada *

Department of Chemistry, Tokyo Institute of Technology, Meguro-ku, Tokyo 152-8551, Japan

GRAPHICAL ABSTRACT

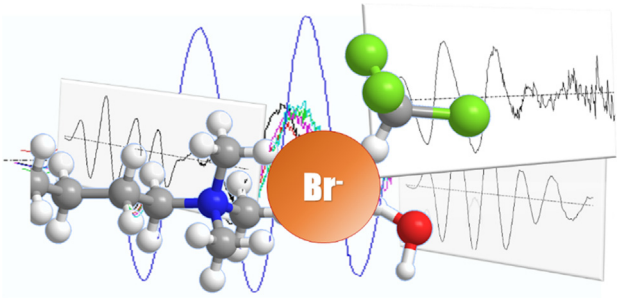

ARTICLE INFO

Article history:
Received 24 March 2021
Revised 12 April 2021
Accepted 13 April 2021
Available online 17 April 2021

Keywords:
Reverse micelle interface
Hexadecyltrimethylammonium bromide
X-ray spectrometry
Chloroform
Hexanol/heptane
Water/surfactant ratio

ABSTRACT

Nanoconfined water exhibits various interesting properties, which are not only of fundamental importance but also of practical use. Because reverse micelles (RMs) provide versatile ways to prepare nanoconfined water, the understanding of their physicochemical properties is essential for developing efficient applications. Although the water properties in the RMs could be affected by its interaction with the RM interface, the details have not been well understood. This study focuses on the local structures of Br^- in hexadecyltrimethylammonium bromide (HTAB) RMs formed in chloroform and 10% hexanol/heptane. The dependence in Br^- hydration on the molar ratio of water to HTAB (w) is investigated using X-ray absorption fine structure (XAFS). These systems cover a wide range of w values (0–30) and allow us to study the impact of this parameter on the local structure of Br^- at the RM interface, which comprises water, surfactant headgroups, and organic solvent components. The presence of multiple scattering paths complicates the XAFS spectra and makes it difficult to analyze them using standard fitting methods. The linear combination of the spectra corresponding to the individual scattering paths captures the molecular processes that occur at the RM interface upon increasing w. The maximum hydration number of Br^- is found to be 4.5 at $w > 15$, suggesting that although most of the ions remain at the interface as partly hydrated ions, some of them dissociate as completely hydrated ones.

1. Introduction

Reverse micelles (RMs) are formed when amphiphilic (surfactant) molecules dissolve in an organic solvent with a small amount of water. The hydrophilic headgroup of the surfactant molecule interacts with water to form a core, while the hydrocarbon chains extend toward the organic solvent. Nanosized water droplets are

* Corresponding authors.
E-mail addresses: hmakoto@chem.titech.ac.jp (M. Harada), tokada@chem.titech.ac.jp (T. Okada).

https://doi.org/10.1016/j.jcis.2021.04.070
0021-9797/

stably dispersed in the organic solvent and confined in the RM cores surrounded by surfactant molecules [1]. This nanospace has been employed to carry out specific reactions and material syntheses [2–5]. The nanoconfined water in the RM core exhibits interesting features, such as slow dynamic properties, particularly when the size of the RM, which is controlled by the water/surfactant molar ratio (w), is small [6,7]. Thus, the unusual water properties in the RM core are deemed to originate mainly from the interaction of the water molecules with the interface [8–11]. Ionic surfactants, including sodium bis(2-ethylhexyl) sulfosuccinate (AOT) [12–14] and hexadecyltrimethylammonium bromide (HTAB) [14–18], are often used to prepare RMs. The radius of the RM was determined to be 1.26 nm for HTAB RMs in chloroform (w = 3.8) [17], and 2.58 nm (w = 15) and 4.44 nm (w = 35) in hexanol [16]. Because both ionic headgroups and counterions are hydrophilic, their interactions with water can strongly affect the water properties at the RM interface, and this effect should become more marked as w decreases. Thus, the hydration of the surfactant molecules and counterions is expected to be a critical factor controlling the events that occur in RM systems.

Long et al studied the local structure of Br^- in (1*R*,2*S*)-dodecyl (2-hydroxy-1-methyl-2-phenylethyl)dimethylammonium bromide RMs formed in toluene using small-angle X-ray scattering and X-ray absorption fine structure (XAFS) [19]. No interaction between bromide and water was detected for $w < 2$ because Br^- was strongly bound to the surfactant headgroups. In contrast, it is well known that the counterions of normal micelles are partly dissociated from the micelle surface and completely hydrated in the bulk aqueous phase. The partial dissociation of the counterions in normal micellar systems has been confirmed by various methods, including molecular dynamics simulation [20,21], conductometry [22], fluorometry [17], and X-ray spectroscopy [23]. The counterion dissociation causes charging of normal micelles and thus induces a measurable zeta potential at the micelle/solution interface [24]. Because the outer surface of a normal micelle is in contact with a bulk aqueous phase, a sufficient amount of water is available for the complete hydration of the counterions. In contrast, as the amount of water in the RM core is limited, full hydration of the counterions may not be achieved.

We previously studied the hydration structures of counterions in anion- and cation-exchange resins, surface monolayers, normal micelles, and ice-confined spaces using XAFS and revealed various interesting features [25–29]. For example, while water molecules adsorbed by a resin directly hydrated the counterions until the hydration number reached 3, further water adsorption led only to a small increase in the hydration number of the counterion. The maximum hydration number reached 3.9 for Cl^- and 3.4 for Br^-, which were smaller than the hydration number (=6) of the ions in aqueous solution. Excess water was condensed in the interstitial spaces of the resin [26]. Thus, most of the counterions were partially hydrated, and a complete hydration shell was not formed. Partial hydration is a key factor governing the ion-exchange selectivity. A similar ion hydration behavior was confirmed for the counterions of Gibbs monolayers on the solution surface [23,30].

In terms of water availability for ion hydration, the interior of ion-exchange resins is similar to the RM interface. One of the intriguing features of RMs is that the amount of water in the core can be controlled by varying w. As mentioned above, Long et al reported that no hydration was detected for Br^- in the RM core when $w < 2$ [19]. Because the stability of RMs depends on the type of surfactant and organic solvent, higher w values can be explored by considering different RM systems. In this study, we investigate systematic changes in the solvation structure of Br^- in HTAB RMs formed in chloroform and 10% (volume %) hexanol/heptane; w was varied in the range of 0–4 for the former and 5–30 for the latter. In this way, we could explore the Br^- hydration at the HTAB RM interface over a wide range of w (0–30).

2. Experimental section

2.1. Preparation of RM solutions

All reagents were of analytical grade. HTAB was used after drying in vacuum. The water concentration in chloroform was determined to be 11.8 ± 1.3 mM by Karl–Fischer titration, whereas that in 10% hexanol/heptane was not detected by the same method because of low water concentration. The water concentrations in the original organic solvents were not considered for the determination of w values. The water concentration was not changed by dissolving HTAB in the organic solvent. RM solutions were prepared by adding appropriate amounts of water to the HTAB solution in chloroform or 10% hexanol/heptane. Water was purified using a MilliQ system. The RM solutions were prepared under conditions in which phase separation did not occur, that is, w = 1–4 for 400 mM HTAB RMs in chloroform and $w \geq 5$ for 100 mM HTAB RMs in 10% hexanol/heptane.

2.2. Br K-edge XAFS measurements

All XAFS spectra at the Br *K*-edge were recorded at the BL-12C facility of the Photon Factory, High Energy Accelerator Research Organization (KEK-PF) in Tsukuba, Japan. The monochromator was equipped with an Si(311) channel-cut crystal. The incident and transmitted X-ray intensities were measured with ionization chambers. The samples were sealed in polytetrafluoroethylene (PTFE) or polyethylene pouches and sandwiched between Cu holders. The sample thickness was adjusted in such a way to obtain an appropriate signal jump at the Br *K*-edge. XAFS measurements were carried out at room temperature (*ca.* 25 °C). The scattering amplitudes and phase shifts of the model systems were calculated using the FEFF8.20 program. The details of the XAFS spectral analysis are described in the Supporting Information [31].

3. Results and discussion

3.1. XAFS analysis of the local structures of Br^- in HTAB RMs with w = 0–4 formed in chloroform

Fig. 1 shows the XAFS $\chi(k)$ spectra at the Br *K*-edge for the HTAB RMs with w = 0–4. The spectrum for hydrated Br^- in bulk aqueous solution is also shown for comparison. Although chloroform contained 11 mM water as an impurity, this concentration was not taken into account in the w value because negligible compared to the HTAB concentration (400 mM). For w = 0, HTAB may dissolve in chloroform as neutral molecules (such as ion pairs and aggregates) or dissociate into HTA^+ and Br^-. We measured the conductivity of the HTAB chloroform solution to obtain information on the dissociation of HTAB. The molar conductivity of the 100 mM HTAB chloroform solution was approximately 10 μS cm^{-1}, suggesting that HTAB is hardly dissociated and is dissolved as neutral species. Thus, because chloroform and the trimethylammonium group are expected to be the scattering groups for w = 0, the XAFS spectrum (black curve in Fig. 1) was analyzed using Br—H—C as model. The results of the XAFS analysis are shown in Figure S1 and Table S1. The optimized Br–C coordination length (r) was 3.56 (±0.139) Å, and the coordination number (N) was 8.3 (±6.8); the large error in N arises from the limited quality of the spectrum, due to absorption by the solvent. However, the present spectra maintain qualities high enough to provide the structural information based on a single-shell assumption. The essential issue, which

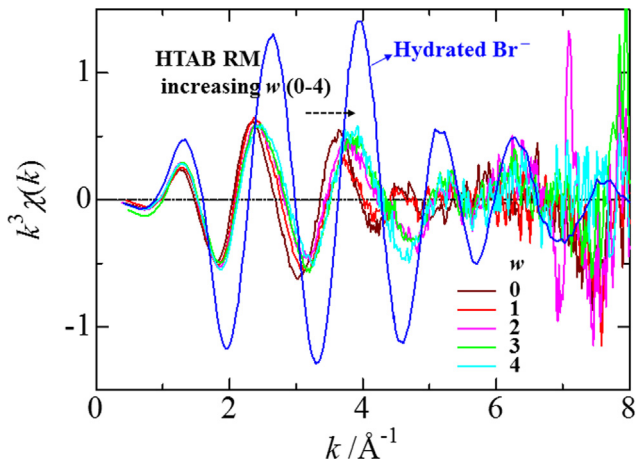

Fig. 1. XAFS spectra of Br^- in HTAB RMs with w = 0–4 (black to light blue) formed in chloroform, along with the spectrum of hydrated Br^- (blue). (For interpretation of the references to colour in this figure legend, the reader is referred to the web version of this article.)

complicates the XAFS spectra for Br^- at the RM interface, is the complex composition of the coordination sphere. Multiple scattering paths lead to a decrease in the oscillation intensity particularly in the large k range. Therefore, the assumption of a single scattering path results in large coordination number and large Debye-Waller factor as listed in Table S1. Unusual results for w = 1 are also explained by the inconsistency between simple Br—H—C model and multiple scattering paths. Thus, this model is inappropriate to describe the spectra with $w \geq 1$. This is caused by the progressive hydration of Br^-, i.e., the main scattering path shifts from Br—H—C to Br—H—O as w increases.

Interestingly, Fig. 1 shows that the oscillation shift of the spectra systematically changes and approaches that of hydrated Br^- as w increases, indicating that this change reflects the progressive hydration of Br^-. However, the oscillation intensity is almost constant over the entire w range, and the oscillation shift is still different from that of hydrated Br^-, suggesting that chloroform and/or the trimethylammonium groups still affect the spectra even for w = 4. In general, the backscattering from water oxygen atoms is much stronger than that from carbon atoms, because of the stronger H-bonding donor ability and the shorter coordination distance of water [25]. The Br—H—O model was also employed for the analysis of the XAFS spectra of the HTAB RMs with w = 1–4. The fitting results are shown in Figure S2, with the parameters summarized in Table S2. The coordination distance ($r_{Br\text{-}O}$) for Br^- in bulk water are well studied using both experimental and theoretical methods. Although XAFS is one of the most reliable experimental method for determining $r_{Br\text{-}O}$, structural parameters depend on the system, model, and analysis method employed. In actuality, reported $r_{Br\text{-}O}$ values vary in the range of 3.19–3.44 Å [19]. [25,32–35] D'Angelo et al. [34,35] showed that DFT-based molecular dynamics is efficient for analyzing XAFS spectra of solvated Br^- and also that the asymmetric shell for Br^- in methanol provided more reliable $r_{Br\text{-}O}$ (=3.4 Å) value than the Gaussian shell ($r_{Br\text{-}O}$ = 3.28 Å). Thus, the $r_{Br\text{-}O}$ value strongly depends on the model and method used for the XAFS data analysis. The difference in oscillation shift between the experimental and fitted spectra is significant for w = 1, but becomes smaller for $w \geq 2$. In addition, the Br-O distance for w = 1 ($r_{Br\text{-}O}$ = 3.67 Å) is obviously anomalous, whereas the values for $w \geq 2$ ($r_{Br\text{-}O}$ ~ 3.2 Å) are in agreement with the Br–O distance of hydrated Br^-. This indicates that water coordination becomes dominant for $w \geq 2$, while for w = 1 the effects of chloroform and the surfactant headgroups outweigh that of water and thus Br—H—O is not an appropriate model. The simultaneous coordination of water, chloroform, and the headgroup should be taken into account to draw a more accurate molecular picture of Br^- ions at the RM interface. However, multishell XAFS analyses could not be applied because of the limited k range originating from the intrinsically long coordination distance of Br^-, and also because of the limited quality of the spectra. Thus, a different approach is necessary to obtain further information on the interfacial structure.

3.2. Analysis considering multiple scattering paths

We previously showed that the analysis discussed below is effective for ions with multiple scattering paths [23,26]. The counterions in RMs are electrostatically bound to the headgroups of the surfactant molecules and can be simultaneously hydrated [36]. In addition, organic solvent molecules can penetrate the hydrocarbon layer and interact with the counterions [37]. Therefore, three scattering paths can be involved in the present system, as schematically shown in Fig. 2. In this case, the XAFS spectrum (χ) is given by the linear combination of the spectra corresponding to the individual scattering paths (χ_1, χ_2, and χ_3).

$$\chi = \alpha\chi_1 + \beta\chi_2 + \gamma\chi_3 \quad (1)$$

where α, β, and γ represent the contributions from χ_1, χ_2, and χ_3, respectively. Because one scattering group is represented by water, the spectrum of hydrated Br^- is suitable as one component of the spectrum (χ_1). The second scattering group is the trimethylammonium group of the surfactant molecule. In the crystal structure of dodecyltrimethyl ammonium bromide, Br^- is coordinated by four trimethylammonium groups in a fourfold planar configuration [38]. Although this structure is not maintained at the RM interface, Br^- can be surrounded by headgroups in a two-dimensional arrangement. In fact, a simulation study of sodium and potassium counterions in AOT RMs suggested that the headgroups and counterions make up the RM interfacial sphere together with water molecules [36]. Therefore, the spectrum of the HTAB crystal (Figure S3) was selected as χ_2 because it likely represents the effect of the trimethylammonium groups.

Br^- salts are not fully dissociated in chloroform of low permittivity and polarity [39]. As discussed above, conductivity measurements indicated that HTAB dissolves in chloroform as neutral species, without dissociating into ions. Thus, the XAFS spectrum of chloroform-solvated Br^- cannot be measured directly. As discussed earlier, the spectrum for w = 0 involves simultaneous scatterings from the trimethylammonium group and chloroform; this

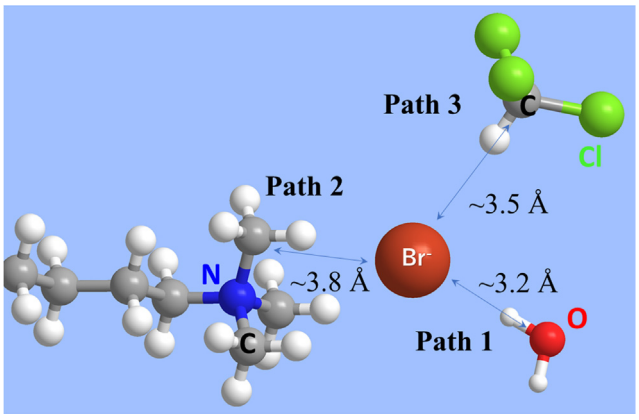

Fig. 2. Schematic representation of three possible scattering paths for the HTAB RM in chloroform.

spectrum was selected as χ_3. Hence, the scattering from the trimethylammonium group contributes to both the second and third terms of Eq. (1).

Fig. 3 compares the spectra for w = 1–4 with the fitting results obtained using Eq. (1). To avoid effects of the limited spectral quality, the fitting was applied to the range of k = 1.8–6 Å^{-1}. All experimental spectra were well reproduced by the regression analysis. Although XAFS analyses should be carried out in wider k ranges, the present method allows us to extract structural information from the limited spectral range, where the principal characteristics of the coordination shell are well seen. The changes in the α, β, and γ parameters with w are summarized in Fig. 4. The spectrum for w = 1 is almost fully accounted for by the γ factor (=0.75 ± 0.23) with a small contribution from α (0.13 ± 0.09). This strongly suggests that the local structure corresponding to w = 0 is almost maintained for w = 1, and only a small number of chloroform molecules in the coordination sphere of Br^- are replaced by water. Klicova et al. reported that HTAB forms two different aggregates in chloroform, depending on the concentration [18]. Premicelles are first formed in the millimolar concentration range, and then spherical RMs are obtained when the concentration is increased to approximately 50 mM. The authors found this behavior by determining the critical micelle concentration (CMC) using NMR and conductometry measurements. In a subsequent study we confirmed that, because the premicelles and spherical RMs have the same solute partitioning ability, they also have a similar nature

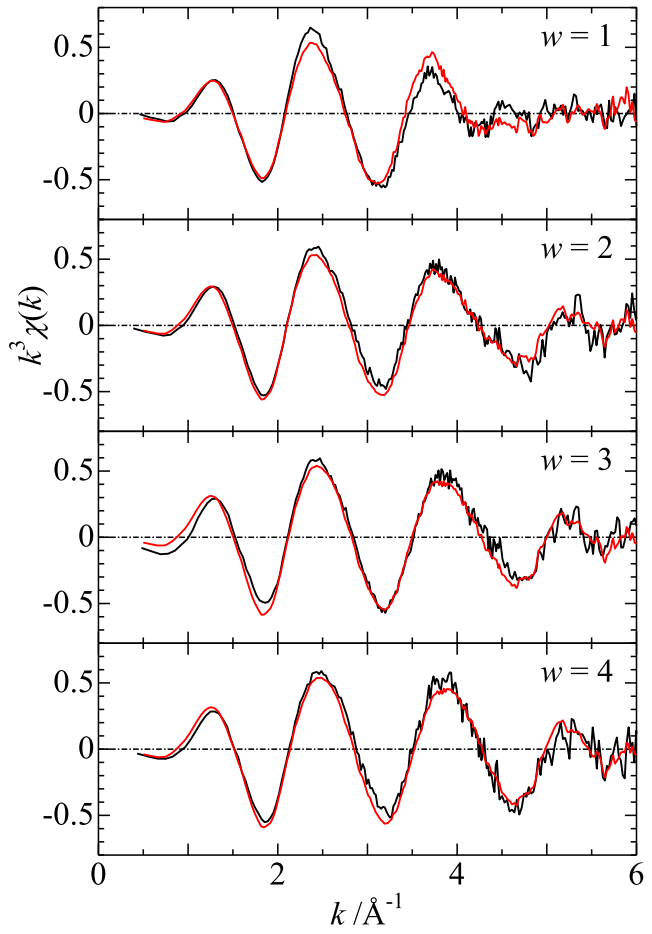

Fig. 3. XAFS spectra for Br^- ions in HTAB RMs formed in chloroform. Black and red curves represent experimental $k^3\chi$ spectra and fits obtained using Eq. (1), respectively. Fittings were applied to the spectra in the range of k = 1.8–6 Å^{-1}. (For interpretation of the references to colour in this figure legend, the reader is referred to the web version of this article.)

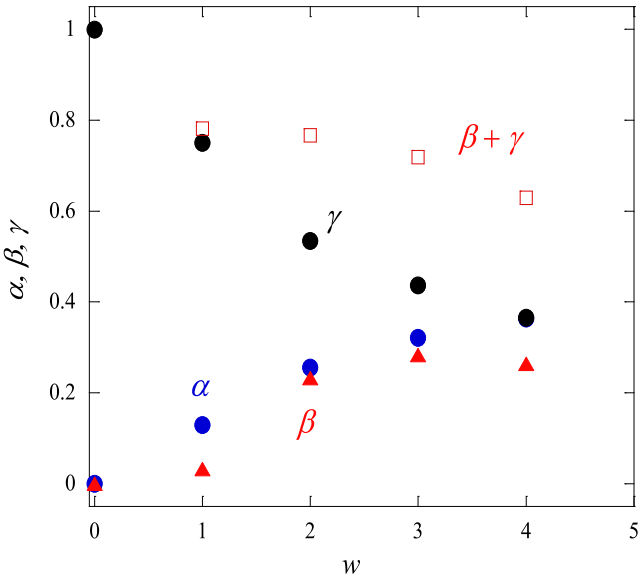

Fig. 4. Changes in α, β, and γ parameters with w in HTAB RM formed in chloroform, as determined using Eq. (1). The standard deviations for α, β, and γ are 0.09, 0.33, and 0.23, respectively.

in this context [40]. The access of chloroform to Br^- is largely restricted for spherical RMs compared to open premicelles, as illustrated in Fig. 5. Chloroform molecules can easily approach Br^- in premicelles because of their low steric barrier. Hence, the large γ contribution for w = 1 suggests that premicelles are still a dominant species in this medium. In addition, similar spectral features for w = 0 and 1 imply that premicelles are formed for w = 0 and enhance the HTAB solubility in chloroform.

Fig. 4 shows that, as w increases, α and β increase while γ significantly decreases. Thus, chloroform molecules are expelled from the solvation shell of Br^- as the hydration proceeds. The Gibbs energy of transfer for chloroform from hexane, which represents the hydrocarbon layer, to water was determined to be 5.7 kJ mol^{-1} based on the distribution coefficient. Thus, the access of chloroform molecules to Br^- is largely restricted in the spherical RMs, where chloroform molecules must penetrate the hydrocarbon layer and reach the RM interface in order to interact with Br^-. Therefore, the continuous decrease in γ implies the formation of spherical RMs. The coordination of the surfactant headgroup contributes to both β and γ. Therefore, (β + γ) can be a good measure representing the contribution of the headgroup. As shown in Fig. 4, (β + γ) decrease with increasing w; thus, the contribution of the headgroup becomes weaker. This suggests that Br^- is drawn into the water core of the RM when the water content increases. Therefore, the interactions of Br^- with chloroform and the trimethylammonium group become weaker with increasing w.

3.3. Local structures of Br^- in HTAB RMs with $w \geq 5$

Fig. 6 shows the XAFS spectra at the Br K-edge for HTAB RMs in 10% hexanol/heptane, with w varying from 5 to 30. The spectra of hydrated Br^- and crystalline HTAB are also displayed for comparison. RMs with such high water contents cannot be prepared in chloroform: the water phase is separated from the organic phase. In contrast, stable RMs (no phase separation occurs) are formed in 10% hexanol/heptane, where hexanol acts as a cosurfactant [15,16]. Interestingly, the oscillation structures are similar to those of hydrated Br^- over the entire w range studied, suggesting that water molecules coordinate Br^- at the RM interface and act as the main scattering path even at w = 5. A small shift of the

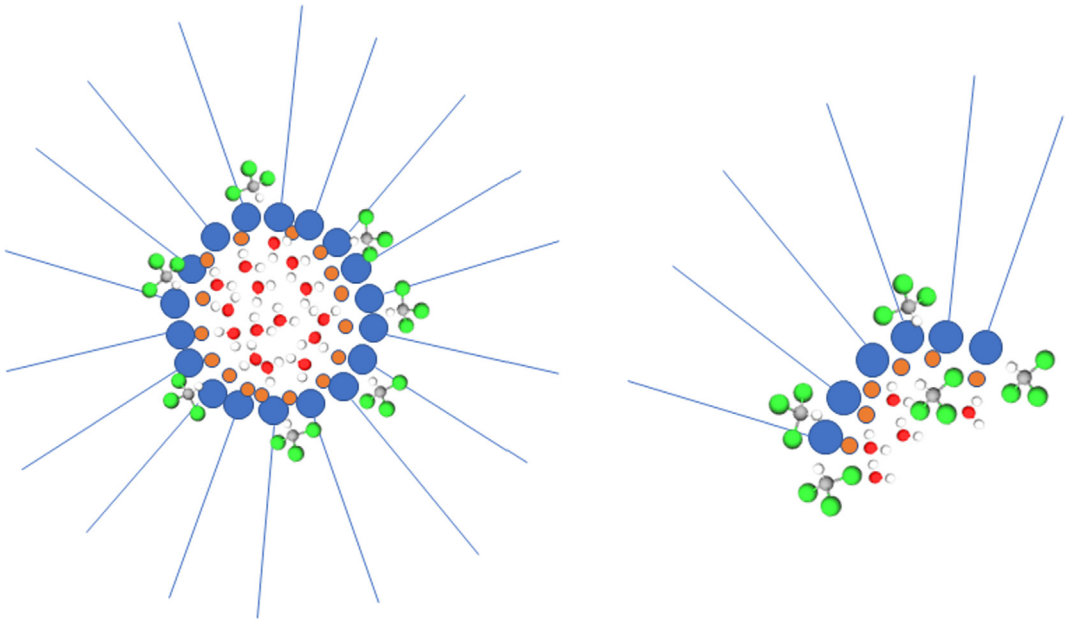

Fig. 5. Schematic representation of RM in chloroform (left) and premicelle (right). The hydrocarbon chain and headgroup of the HTAB molecule are represented as lines and blue solid circles, respectively; brown circles represent Br^-. (For interpretation of the references to colour in this figure legend, the reader is referred to the web version of this article.)

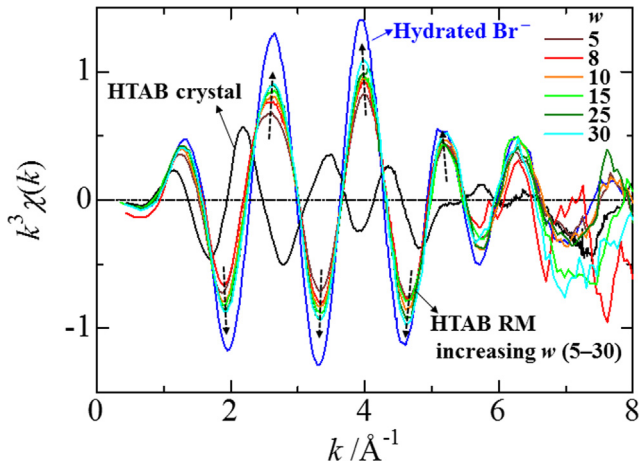

Fig. 6. XAFS spectra of Br^- in HTAB RMs with w = 5–30 formed in 10% hexanol/heptane, along with the spectra of hydrated Br^- and crystalline HTAB.

oscillation phase occurs upon increasing w, accompanied by a significant increase in the oscillation intensity. The spectra shown in Fig. 6 were analyzed using Br—H—O as model. The XAFS curve-fitting results are shown in Figure S4, and the fitting parameters are summarized in Table S3. The coordination distance is 3.1–3.2 Å in all cases, which is a strong indication of water coordination [25,32]. In addition, N increases with increasing w to 15 and remains almost constant at 3.5 for further increase in w. Thus, a hydration shell is not fully formed around Br^- even when w reaches 30. This confirms the strong interaction between the headgroups and Br^-.

As already stated, the XAFS parameters, $r_{Br\text{-}O}$, N, and the Debye-Waller factor (σ), show variations depending on model and analysis methods and also have intercorrelations. Antalek et al. [33] studied the hydration structures of halide ions using XAFS and Minuit X-ray absorption near edge analyses and showed that r increases with increasing N. Also, it is well known that there is a correlation between N and σ for hydrated ions [41]. Thus, the XAFS parameters correlate with each other for hydrated halide ions in bulk water. By contrast, the coordination sphere of Br^- at the RM interface is occupied by several different groups, including water, organic solvent, and surfactant headgroup, as discussed above. Since the XAFS oscillation due to water coordination outweighs those of the latter two groups because of the shorter coordination distance of the former and the larger backscattering ability of an oxygen atom than carbon atoms, the hydration number dominantly determines the N value. However, the organic solvent and surfactant headgroup remain in the coordination shell of Br^- even for large w values. Although these groups affect the N value determined using Br—H—O model to some extent, their contributions become smaller as hydration proceeds. Therefore, an increase in N with increasing w approximately represents an increase in the hydration number. However, the actual coordination number should be larger than N, because weak-scattering groups still exist on the coordination sphere. An increase in N has negligible impacts on $r_{Br\text{-}O}$ because water is the main scattering path, and also a small effect on σ values because an increase in w do not cause a large change in the crowding of the solvation sphere of Br^- at the RM interface.

The spectra shown in Fig. 6 were further analyzed using Eq. (1) to clarify the effects of multiple scattering paths. However, because HTAB is insoluble in 10% hexanol/heptane, the spectrum of Br^- coordinated by the solvent (corresponding to the χ_3 parameter for the spectra in chloroform) could not be obtained. The low solubility of HTAB in this solvent implies its weak solvation ability at the RM interface. In addition, although hexanol may coordinate Br^- at the RM interface, XAFS cannot distinguish this contribution clearly from that of hydration. Thus, Equation (1) can be simplified to the following form, in which the scattering paths are those of water and trimethylammonium:

$$\chi = \alpha\chi_1 + \beta\chi_2 \quad (2)$$

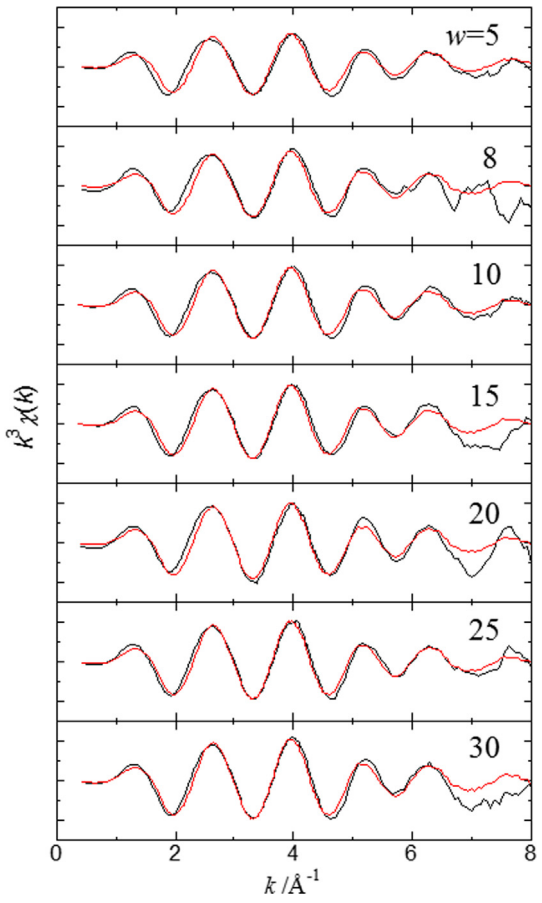

Fig. 7. XAFS spectra of Br^- in HTAB RMs formed in 10% hexanol/heptane. Black and red curves denote experimental $k^3\chi$ spectra and fits using Equation (2), respectively. (For interpretation of the references to colour in this figure legend, the reader is referred to the web version of this article.)

Fig. 7 summarizes the results of the fitting based on Eq. (2). The experimental XAFS spectra are well reproduced by the linear combination of the spectra of hydrated Br^- and crystalline HTAB, indicating that the assumption of two scattering paths is appropriate.

Fig. 8 shows the changes in α and β as a function of w. For $w < 15$, α increases but β significantly decreases. These changes become smaller with further increases in w, until the two parameters stay almost constant at $\alpha = 0.78$ and $\beta = 0.2$. The structure of the coordination shell of Br^- hardly changes for $w \geq 15$; under these conditions, the bromide ions reach a stable local structure and the added water molecules are accommodated in the aqueous core, without modifying the interfacial structure of Br^-. The decrease in β with w indicates that the coordination of the trimethylammonium group becomes weaker with increasing w. As discussed in detail below, the hydration number of Br^- reaches 4.5 at $w \geq 15$, according to the analyses based on Eq. (2). If Br^- and surfactant headgroups are positioned on the interfacial plane, Br^- cannot be coordinated by 4.5 water molecules, because of the insufficient space to form the hydration shell. Therefore, Br^- should be drawn into the water core in order to interact with 4.5 water molecules.

3.4. Hydration of Br^- in the water core

Fig. 9 summarizes the dependence of the Br^- hydration number (N_{hydr}) on w, where we assumed $N_{hydr} = 6\alpha$, because a number of studies suggested that the hydration number of Br^- in bulk water is approximately 6 [32,42,43]. As discussed above, the interfacial

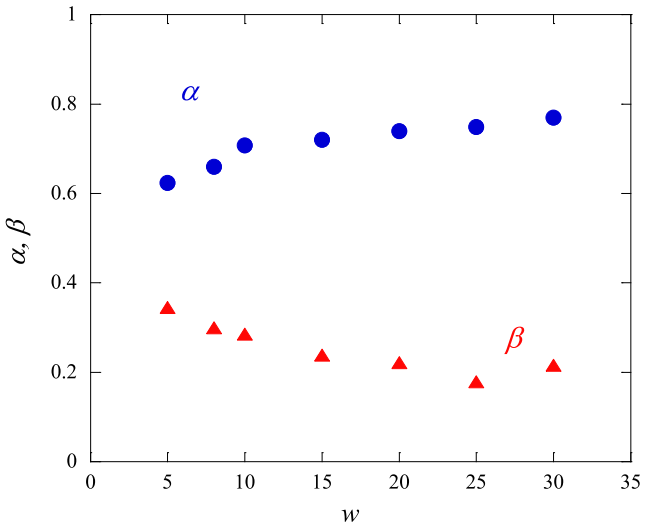

Fig. 8. Changes in α and β parameters obtained for the RMs formed in 10% hexanol/heptane as a function of w. The values were determined from Eq. (2). The standard deviations for α and β are 0.11 and 0.37, respectively.

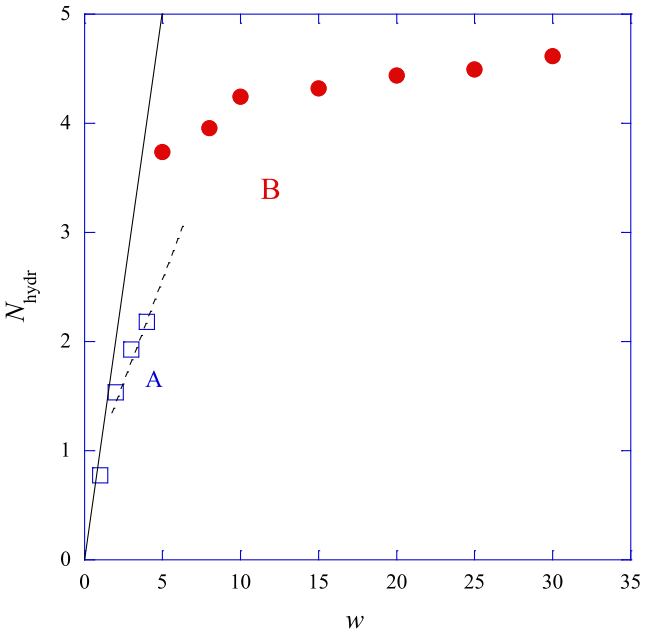

Fig. 9. Change in the hydration number (N_{hydr}) with w for the RMs formed in chloroform (A) and 10% hexanol/heptane (B). The solid and broken lines represent the $N_{hydr} = w$ relation and the extrapolation for N_{hydr} in chloroform.

structure for the RMs in chloroform is not the same as that in hexanol/heptane. However, to understand the general trend, the 6α values determined for these RMs are plotted in Fig. 9. For $w < 5$, the hydration number is almost proportional to w, indicating that water molecules predominantly hydrate Br^-. In particular, for $w \leq 2$, 6α is almost equal to w; all water molecules added to the system solvate Br^-. However, a further increase in w results in a small increase in N_{hydr}, because no more water molecules participate in the hydration of Br^-. Eventually, N_{hydr} stays almost constant at 4.5 for $w > 10$. In any case, the effect of the surfactant headgroup was observed in the XAFS spectra, which indicated that the complete hydration shell is not formed even after supplying a sufficient amount of water.

The changes in the coordination shell structure of Br^- are schematically illustrated in Fig. 10. In the RM formed in chloroform, the solvent is obviously involved in the solvation sphere of Br^-. An increase in w facilitates hydration of $Br^-$and simultaneously reduces the interaction with chloroform. Then, Br^- is drawn toward the RM core, and its interaction with the headgroup also becomes weaker. Although each Br^- ion simultaneously interacts with multiple headgroups when located on the interfacial plane, such interaction becomes difficult to establish if the ion is drawn into the core and located away from the interfacial plane, as illustrated in Fig. 10.

In 10% hexanol/heptane, solvation by the organic solvents could not be clearly confirmed because of the difficulty in distinguishing hexanol OH groups from water. Fuglestad et al studied HTAB RMs in hexanol using small-angle X-ray/neutron scattering and molecular dynamics simulations [15,16]. They found a significant penetration of the hexanol OH groups into the hydrocarbon layer of the RM, as well into the interfacial region. This suggests that hexanol may contribute to the α parameter. The plots for 10% hexanol/heptane in Fig. 8 show slightly higher values than those extrapolated for chloroform. This difference may reflect the contribution from hexanol OH groups. The simulations by Fuglestad et al show that the penetration of hexanol OH groups can be detected, but is not significant. We analyzed the solvation structure of Br^- in methanol using XAFS measurements; the results revealed that the r value is similar to that obtained in water, whereas the N parameter (3.5) is significantly smaller than that measured in water (6) [25]. This results in the low oscillation intensity for Br^- in methanol. Therefore, the coordination of hexanol to Br^- is much weaker than that of water. Whereas the coordination of hexanol significantly contributes to the XAFS spectrum when only an insufficient amount of water is available for hydration, its influence becomes marginal with increasing water concentration. Hence, hydration is the main factor determining the value of α for larger w values.

The maximum hydration number of Br^- was determined to be 3.9 for an anion-exchange resin [26] and 4.2 for a normal HTAB micelle [23] using a similar approach. The corresponding value determined for the RM studied in the present work is 4.5. This value is slightly larger that of the normal micelle. This suggests that water confined in the RM has bulk-like properties for $w > 15$. A number of studies have been conducted to reveal the properties of water confined in RMs. For example, IR spectroscopic studies showed that more than 50% of water molecules become

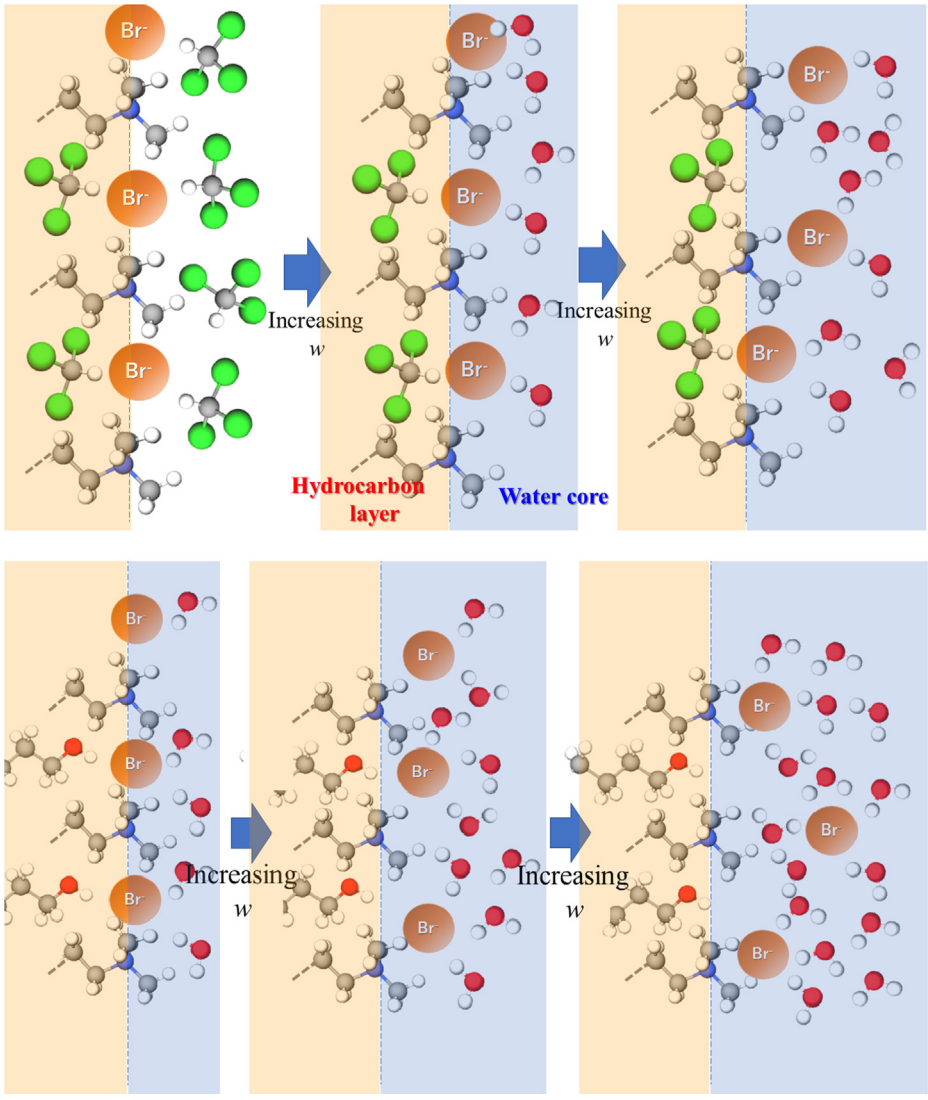

Fig. 10. Schematic representation of changes in the solvation structure of Br^- at the interfaces of RMs formed in chloroform (top) and 10% hexanol/heptane (bottom) as the hydration proceeds. The hydrocarbon chain of the HTA^+ molecule is omitted for clarity.

bulk-like for $w > 10$ and also that the dynamics of water in RMs exhibits bulk-like values when $w > 12$ [7,8]. Also, electron spin resonance indicated that the isotropic to anisotropic change in the spectra is observed at $w \sim 10$ [44]. Thus, the water properties in the RM core change at $w \sim 10$ and become bulk-like when w exceeds this threshold, which almost corresponds to the critical value found in the present work. Although the penetration of the hexanol OH groups can result in a slightly larger hydration number in the RM, this effect is not significant for large w values, as discussed above. The formation of the hydration shell is not complete, and Br^- ions mostly associate with the headgroup even at such high water contents. However, we cannot exclude the possibility that some of the counterions are completely hydrated and dissociated from the headgroup. Further studies using different approaches would be required to determine whether the ions are partly dissociated or not.

4. Conclusion

Br^- at the RM interface is coordinated by water, surfactant headgroups, and organic solvent molecules, and adopts complex local structures, which could not be revealed only by usual XAFS fitting procedure. XAFS analyses based on Equation (1) provided useful information on the local structure of Br^- in RMs with varying w. Interestingly, Br^- is not fully hydrated at the RM interface even when a sufficient amount of water is available, e.g. $w = 30$. Although the present approach is particularly powerful to study complex coordination structures, usual XAFS fitting should also be employed because these methods provide complementary information: for instance, Eq. (1) successfully separates the contributions of different paths but does not provide information on coordination distances and Debye–Waller factors. The fluorescence detection mode may improve the spectral quality arising from the interference of the solvent and is expected to reinforce the conclusions drawn in this work.

The present model assumed an idealized situation of the RM interface and did not take into account the effects of the RM shape and size, the dissolution of organic solvents in the RM cores, escape of water molecules from the RM core, rigidity of the RM interface [45] etc. In actuality, it was indicated that water property depends on the size or curvature of the RM [46,47]. Because we focus our attention on hydration of Br^- in the present paper, the conclusions are not influenced severely by the validity of a model.

Molecular simulations are effective for revealing dynamic and structural features of phenomena in condensed phases, including solvation of ions [33,35]. Such approaches have often been employed to analyze complex systems such as micelles and RMs [1,15,17,37,48]. The present study provides novel experimental evidence on the coordination structure of Br^- at the RM interface and its dependence on w. These results are expected to encourage theoretical scientists to devise new ideas for fully explaining the phenomena that occur in complex systems such as RMs.

CRediT authorship contribution statement

Makoto Harada: Methodology, Validation, Investigation. **Hinako Sakai:** Methodology, Validation, Investigation. **Yu Fukunaga:** Software, Validation. **Tetsuo Okada:** Conceptualization, Supervision, Writing - review & editing.

Declaration of Competing Interest

The authors declare that they have no known competing financial interests or personal relationships that could have appeared to influence the work reported in this paper.

Acknowledgment

This work was supported by the Grant-in-Aid for Scientific Research from the Japan Society for Promotion of Science. This work was performed under the approval of the Photon Factory Advisory Committee (Proposal Nos. 2017G622, 2019G689, and 2019G690).

Appendix A. Supplementary data

Supplementary data to this article can be found online at https://doi.org/10.1016/j.jcis.2021.04.070.

References

[1] G. Eskici, P.H. Axelsen, The size of AOT reverse micelles, J. Phys. Chem. B 120 (2016) 11337–11347.
[2] M. Hojo, R. Kato, A. Narutaki, T. Maeda, Y. Uji-yie, Nitration of phenols in reversed micelle systems and enhanced oxidation ability of dilute nitric acid (less than 2.0 Molarity) in concentrated salt solutions, J. Mol. Liq. 163 (2011) 161–169.
[3] B. Kar, S. Bardhan, P. Ghosh, B. Ganguly, K. Kundu, S. Sarkar, B.K. Paul, S. Das, A fast and additive free C-C homo/cross-coupling reaction in reverse micelle: an understanding of role of surfactant, water content and base on the product yield and reaction site, ChemistrySelect 2 (2017) 1079–1088.
[4] V. Petrov, C.A.T. Laia, F. Pina, Photochromism of 7,4'-dihydroxyflavylium in an AOT reversed micelle system, Langmuir 25 (2009) 594–601.
[5] V. Uskokovic, M. Drofenik, Synthesis of materials within reverse micelles, Surf. Rev. Lett. 12 (2005) 239–277.
[6] J.-B. Brubach, A. Mermet, A. Filabozzi, A. Gerschel, D. Lairez, M.P. Krafft, P. Roy, Dependence of water dynamics upon confinement size, J. Phys. Chem. B 105 (2001) 430–435.
[7] D.S. Venables, K. Huang, C.A. Schmuttenmaer, Effect of reverse micelle size on the librational band of confined water and methanol, J. Phys. Chem. B 105 (2001) 9132–9138.
[8] E.E. Fenn, D.B. Wong, C.H. Giammanco, M.D. Fayer, Dynamics of water at the interface in reverse micelles: measurements of spectral diffusion with two-dimensional infrared vibrational echoes, J. Phys. Chem. B 115 (40) (2011) 11658–11670.
[9] D.E. Moilanen, N.E. Levinger, D.B. Spry, M.D. Fayer, Confinement or the nature of the interface? Dynamics of nanoscopic water, J. Am. Chem. Soc. 129 (2007) 14311–14318.
[10] J. Yang, C. Tang, Y. Wang, C. Chang, J. Zhang, J. Hu, J. Lu, The terahertz dynamics interfaces to ion-lipid interaction confined in phospholipid reverse micelles, Chem. Commun. 55 (100) (2019) 15141–15144.
[11] S.S. Quintana, R.D. Falcone, J.J. Silber, N.M. Correa, Comparison between two anionic reverse micelle interfaces: the role of water-surfactant interactions in interfacial properties, ChemPhysChem 13 (2012) 115–123.
[12] K.J. Blackshaw, M.G. Varmecky, J.D. Patterson, Interfacial structure and partitioning of nitrate ions in reverse micelles, J. Phys. Chem. A 123 (2019) 336–342.
[13] J. Moon, M. Nilsson, Coordination chemistry of lanthanides in a AOT-CMPO solvent extraction system: UV-Vis and XAFS studies, Dalton Trans. 47 (2018) 15424–15438.
[14] J. Luo, Y. Liu, S. Yang, Different locations of adenine in AOT and CTAB reverse micelles, J. Mol. Liq. 232 (2017) 236–242.
[15] B. Fuglestad, K. Gupta, A.J. Wand, K.A. Sharp, Characterization of cetyltrimethylammonium bromide/hexanol reverse micelles by experimentally benchmarked molecular dynamics simulations, Langmuir 32 (2016) 1674–1684.
[16] B. Fuglestad, K. Gupta, A.J. Wand, K.A. Sharp, Water loading driven size, shape, and composition of cetyltrimethylammonium/hexanol/pentane reverse micelles, J. Colloid Interface Sci. 540 (2019) 207–217.
[17] L. Klicova, E. Muchova, P. Sebej, P. Slavicek, P. Klan, Nature of CTAB/water/chloroform reverse micelles at above- and subzero temperatures studied by nmr and molecular dynamics simulations, Langmuir 31 (2015) 8284–8293.
[18] L. Klicova, P. Sebej, P. Stacko, S.K. Filippov, A. Bogomolova, M. Padilla, P. Klan, CTAB/water/chloroform reverse micelles: a closed or open association model?, Langmuir 28 (2012) 15185–15192.
[19] A. Longo, F. Giannici, G. Portale, D. Banerjee, P. Calandra, V. Turco Liveri, Morphology and Local Organization of Water-Containing (1R,2S)-Dodecyl(2-Hydroxy-1-Methyl-2-Phenylethyl)Dimethylammonium Bromide Reverse Micelles Dispersed in Toluene, J. Chem. Phys. 141 (2014) 084904.
[20] C.D. Chrystal, D. Bruce, M.L. Berkowitz, L. Perera, M.D.E. Forbes, Molecular dynamics simulation of sodium dodecyl sulfate micelle in water: micellar structural characteristics and counterion distribution, J. Phys. Chem. B 106 (2002) 3788–3793.
[21] M. Jorge, Molecular dynamics simulation of self-assembly of n-decyltrimethylammonium bromide micelles, Langmuir 24 (2008) 5714–5725.
[22] M. Pérez-Rodríguez, G. Prieto, C. Rega, L.M. Varela, F. Sarmiento, V. Mosquer, A comparative study of the determination of the critical micelle concentration

by conductivity and dielectric constant measurements, Langmuir 14 (1998) 4422–4426.
[23] M. Harada, H. Satou, T. Okada, Hydration structures of bromides on cationic micelles, J. Phys. Chem. B 111 (2007) 12136–12140.
[24] D. Zadaka, A. Radian, Y.G. Mishael, Applying zeta potential measurements to characterize the adsorption on montmorillonite of organic cations as monomers, micelles, or polymers, J. Colloid Interface Sci. 352 (2010) 171–177.
[25] M. Harada, T. Okada, I. Watanabe, Solvation structure of bromide ion in anion-exchange resins, J. Phys. Chem. B 106 (2002) 34–40.
[26] T. Okada, M. Harada, Hydration of halide anions in ion-exchange resin and their dissociation from cationic groups, Anal. Chem. 76 (2004) 4564–4571.
[27] M. Harada, T. Okada, Hydration of counterions in cation exchange resins studied by X-ray absorption fine structure, Chem. Commun. 5182–5184 (2008).
[28] M. Harada, T. Okada, Local structures of ions at ion-exchange resin/solution interface, J. Chromatogr. A 1085 (2005) 3–7.
[29] Y. Tasaki, M. Harada, T. Okada, Eutectic transition of local structure for bromide ion in bulk and on surface of doped ice, J. Phys. Chem. C 114 (2010) 12573–12579.
[30] M. Harada, T. Okada, I. Watanabe, X-ray absorption fine structure of ions attracted by a zwitterionic surface monolayer, J. Phys. Chem. B 107 (2003) 2275–2280.
[31] H. Sakane, T. Miyanaga, I. Watanabe, N. Matsubayashi, S. Ikeda, Y. Yokoyama, Reproducibility tests of extended X-Ray absorption fine structure for aqua and ammine complexes of first transition metals in solid and aquesou solution, Jpn. J. Appl. Phys. 32 (1993) 4641–4647.
[32] S.L. Wallen, B.J. Palmer, D.M. Pfund, J.L. Fulton, Hydration of bromide ion in supercritical water: an X-ray absorption fine structure and molecular dynamics study, J. Phys. Chem. A 101 (1997) 9632–9640.
[33] M. Antalek, E. Pace, B. Hedman, K.O. Hodgson, G. Chillemi, M. Benfatto, R. Sarangi, P. Frank, Solvation structure of the halides from X-ray absorption spectroscopy, J. Chem. Phys. 145 (4) (2016) 044318.
[34] P. D'Angelo, A. Di Nola, M. Mangoni, N.V. Pavel, An extended X-ray absorption fine structure study by employing molecular dynamics simulations: bromide ion in methanolic solution, J. Chem. Phys 104 (1996) 1779–1790.
[35] P. D'Angelo, V. Migliorati, L. Guidoni, Hydration properties of the bromide aqua ion: the interplay of first principle and classical molecular dynamics, and X-ray absorption spectroscopy, Inorg. Chem. 49 (2010) 4224–4231.
[36] J. Faeder, M.V. Albert, B.M. Ladanyi, Molecular dynamics simulations of the interior of aqueous reverse micelles: a comparison between sodium and potassium counterions, Langmuir 19 (2003) 2514–2520.
[37] S. Abel, N. Galamba, E. Karakas, M. Marchi, W.H. Thompson, D. Laage, On the structural and dynamical properties of DOPC reverse micelles, Langmuir 32 (41) (2016) 10610–10620.
[38] K. Szulzewsky, B. Schulz, D. Vollhardt, The crystal structure of dodecyltrimethylammoniumbromide, Cryst. Res. Technol. 18 (1983) 1003–1008.
[39] K. Iseda, K. Kokado, K. Sada, Direct detection of the ion pair to free ions transformation upon complexation with an ion receptor in non-polar solvents by using conductometry, ChemistryOpen 7 (2018) 269–274.
[40] H. Sakai, M. Harada, T. Okada, Reverse micelle chromatography for evaluation of partition of organic solutes to micellar pseudophases, J. Colloid Interface Sci. 577 (2020) 191–198.
[41] H. Ohtaki, T. Radnai, Structure and dynamics of hydrated ions, Chem. Rev. 93 (1993) 1157–1204.
[42] G. Licheri, G. Piccaluga, G. Pinna, X-ray diffraction study of LiBr aqueous solutions, Chem. Phys. Lett. 35 (1975) 119–123.
[43] A.H. Narten, Diffraction pattern and structure of aqueous ammonium halide solutions, J. Phys. Chem. A 74 (1973) 765–768.
[44] G. Haering, P.L. Luisi, H. Hauser, Characterization by electron spin resonance of reversed micelles consisting of the ternary system AOT-isooctane-water, J. Phys. Chem. B 92 (1988) 3574–3581.
[45] Sunaina, S.K. Mehta, A.K. Ganguli, S. Vaidya, Small-angle X-ray scattering as an effective tool to understand the structure and rigidity of the reverse micelles with the variation of surfactant, J. Mol. Liq. 326 (2021).
[46] B.L. Bales, A Definition of the degree of ionization of a micelle based on its aggregation number, J. Phys. Chem. B 105 (2001) 6798–6804.
[47] P.A. Pieniazek, Y.-S. Lin, J. Chowdhary, B.M. Ladanyi, J.L. Skinner, Vibrational spectroscopy and dynamics of water confined inside reverse micelles, J. Phys. Chem. B 113 (2009) 15017–15028.
[48] A.V. Martinez, L. Dominguez, E. Malolepsza, A. Moser, Z. Ziegler, J.E. Straub, Probing the structure and dynamics of confined water in AOT reverse micelles, J. Phys. Chem. B 117 (2013) 7345–7351.